Research Article Vol. 38, No. 3 / March 2021 / Journal of the Optical Society of America B 997

Journal of the Optical Society of America B

OPTICAL PHYSICS

Temporal reflection and refraction of optical pulses inside a dispersive medium: an analytic approach

JUNCHI ZHANG,[1,*] W. R. DONALDSON,[2] AND G. P. AGRAWAL[1,2]

[1]The Institute of Optics, University of Rochester, Rochester, New York 14627, USA
[2]Laboratory for Laser Energetics, University of Rochester, Rochester, New York 14623, USA
*Corresponding author: jzh156@ur.rochester.edu

Received 29 November 2020; revised 12 January 2021; accepted 1 February 2021; posted 2 February 2021 (Doc. ID 416058); published 25 February 2021

We develop an analytic approach for reflection of light at a temporal boundary inside a dispersive medium and derive frequency-dependent expressions for the reflection and transmission coefficients. Using the analytic results, we study the temporal reflection of an optical pulse and show that our results agree fully with a numerical approach used earlier. Our approach provides approximate analytic expressions for the electric fields of the reflected and transmitted pulses. Whereas the width of the transmitted pulse is modified, the reflected pulse is a mirrored version of the incident pulse. When a part of the incident spectrum lies in the region of total internal reflection, both the reflected and transmitted pulses are distorted considerably.

https://doi.org/10.1364/JOSAB.416058

1. INTRODUCTION

Reflection of electromagnetic waves at a temporal boundary has attracted considerable attention in several contexts over the last 20 years [1–11]. Recent examples include reflection in space-time metamaterials [8,9], a change in a beam's direction in an anisotropic medium [10], and reflection at multiple temporal boundaries [11]. Most of these studies have focused on a nondispersive medium and ignored the frequency dependence of the refractive index on each side of the temporal boundary. The dispersive effects were included in a 2015 study [6] that considered the reflection and refraction of optical pulses at a moving boundary. It was found that the spectra of reflected and refracted pulses shifted from the spectrum of the incident pulse in such a way that the reflected part never crossed the boundary, even though all parts of the original pulse moved in the same direction. The conservation of momentum at the temporal boundary was used in Ref. [6] to provide analytic expressions for the spectral shifts induced at the temporal boundary.

Although temporal reflection of optical pulses has been studied extensively in recent years [8–22], it has required extensive numerical simulations because no analytic expressions have yet been found for the reflection and transmission coefficients at a moving temporal boundary inside a dispersive medium.

In this paper, we provide the analytical expressions for these coefficients by solving the problem in the frequency domain and use them to predict the temporal and spectral features of the reflected and refracted pulses. The paper is organized as follows. In Section 2, we discuss momentum conservation and the boundary conditions across a temporal boundary and use them to derive the frequency-dependent reflection and transmission coefficients. In Section 3, we use our analytic expressions to estimate the electric fields of the reflected and transmitted pulses after making suitable, physically justified approximations. These results apply for pulses of arbitrary shapes. We consider two specific cases in Section 4 and discuss how the shapes and spectra of the reflected and refracted pulses are modified for an incident Gaussian pulse depending on the dispersive properties of an optical fiber. We summarize our main results in Section 5.

2. ANALYTIC THEORY OF TEMPORAL REFLECTION

We consider propagation of optical pulses inside a dispersive medium (such as an optical fiber) with the propagation constant $\beta(\omega)$. In the following discussion, we assume that the pulse's spectrum is relatively narrow (quasi-monochromatic approximation), and we can expand $\beta(\omega)$ around a reference frequency in a Taylor series as

$$\beta(\omega) = \beta_0 + \beta_1(\omega - \omega_0) + \frac{1}{2}\beta_2(\omega - \omega_0)^2, \tag{1}$$

where ω_0 is a reference frequency close to the central frequency of the pulse (but it does not have to be the central frequency) and we neglected the third and higher-order dispersive terms. Note that the pulse frequency should be away from any resonant frequencies of the material in order that Eq. (1) holds.

We assume that the pulse is approaching a temporal boundary moving at the speed V_B. The refractive index changes across this boundary by a constant amount Δn, and the propagation constant after the boundary becomes

$$\beta_t(\omega) = \beta_0 + \beta_B + \beta_1(\omega - \omega_0) + \frac{1}{2}\beta_2(\omega - \omega_0)^2, \quad (2)$$

where $\beta_B = \frac{\omega_0}{c}\Delta n$.

The evolution of the pulse across the temporal boundary is governed by the following equation [6] satisfied by the slowly varying envelope $A(z, t)$ of the pulse:

$$\frac{\partial A}{\partial z} + \Delta\beta_1 \frac{\partial A}{\partial t} + i\frac{\beta_2}{2}\frac{\partial^2 A}{\partial t^2} = i\beta_B H(t - T_B)A, \quad (3)$$

where we work in a frame in which the temporal boundary appears stationary, i.e., $t = t' - z/V_B$, where t' is the time in the laboratory frame; $\Delta\beta_1 = \beta_1 - 1/V_B$ is the relative group delay of the pulse in this time frame. In Eq. (3), $H(t - T_B)$ is the Heaviside step function taking the value 1 when $t > T_B$ and 0 when $t < T_B$. T_B is the time delay of the time boundary at the incident plane ($z = 0$). Given the initial pulse shape $A(0, t)$, numerical solutions of Eq. (3) show that the pulse splits into two parts moving at different speeds because of the spectral shifts induced at the boundary [6].

We stress that the velocity V_B is restricted to be subluminal, but it can be larger than the pulse's group velocity. Our problem differs considerably from the case of a nondispersive medium where the refractive index changes everywhere in space at the same time [5,9]. In our case of a moving temporal boundary inside an optical waveguide, spatial distribution of a pulsed optical beam does not change during its propagation. This is the reason why we ignore all spatial effects and solve Eq. (3) with the amplitude $A(z, t)$ specified at $z = 0$. In practice, a moving temporal boundary is often created nonlinearly through the Kerr effect by launching an intense pump pulse into the waveguide.

Our objective is to solve Eq. (3) analytically. The numerical solutions of Eq. (3) indicate that any input pulse is partially reflected and partially transmitted at the temporal boundary such that the two parts have spectra shifted from that of the input pulses. We expect the same to occur for a plane wave. In other words, a plane wave at the frequency $\omega_0 + \Delta\omega$ is also reflected and transmitted at the boundary with different frequency shifts such that the slowly varying amplitude takes this form:

$$A = \begin{cases} e^{i(\beta' z - \Delta\omega t)} + Re^{i(\beta'_r z - \Delta\omega_r t)}, & t < T_B \\ Te^{i(\beta'_t z - \Delta\omega_t t)}, & t > T_B \end{cases}, \quad (4)$$

where R and T are the reflection and transmission coefficients, respectively, that depend on $\Delta\omega$. Here, $\Delta\omega$ is the frequency shift of the input plane wave from the reference frequency ω_0, and $\Delta\omega_r$ and $\Delta\omega_t$ are frequency shifts of the reflected and transmitted plane waves, respectively. These frequency shifts depend on $\Delta\omega$.

We note that Eq. (4) does not violate causality because it is based on plane waves, and the time variable $t = t' - z/V_B$ is defined in a moving frame with t' representing the real time. Causality only requires that the wave packets, representing the reflecting and transmitted parts of the incident pulse, form only after the pulse has arrived at the temporal boundary located at $z_B = T_B/\Delta\beta_1$. As discussed later, this is indeed the case.

We find the frequency shifts $\Delta\omega_r$ and $\Delta\omega_t$ by substituting the solution in Eq. (4) into Eq. (3) for $z < z_B$ and $z > z_B$. This yields the following relations:

$$\begin{cases} \beta'(\Delta\omega) = \Delta\beta_1\Delta\omega + \frac{\beta_2}{2}\Delta\omega^2 \\ \beta'_r(\Delta\omega_r) = \Delta\beta_1\Delta\omega_r + \frac{\beta_2}{2}\Delta\omega_r^2 \\ \beta'_t(\Delta\omega_t) = \beta_B + \Delta\beta_1\Delta\omega_t + \frac{\beta_2}{2}\Delta\omega_t^2 \end{cases}. \quad (5)$$

These are the dispersion relation in the moving frame. From Eq. (3), $A(z, t)$ should be continuous for all values of z. This happens when the three propagation constants are equal, i.e.,

$$\beta' = \beta'_r = \beta'_t. \quad (6)$$

As discussed in Ref. [6], these conditions result from the conservation of momentum in the moving frame. Combining Eq. (5) and Eq. (6), we find two quadratic equations whose solutions determine $\Delta\omega_r$ and $\Delta\omega_t$ with a given $\Delta\omega$. The solution for $\Delta\omega_r$ is found to be

$$\Delta\omega_r = -\frac{2\Delta\beta_1}{\beta_2} - \Delta\omega. \quad (7)$$

The solution for $\Delta\omega_t$ is a more complicated and is given by [6]

$$\omega_t = -\frac{\Delta\beta_1}{\beta_2} + \frac{1}{\beta_2}\sqrt{(\Delta\beta_1 + \beta_2\Delta\omega)^2 - 2\beta_2\beta_B}. \quad (8)$$

To find the reflection and transmission coefficients, R and T, respectively, we make use of the temporal boundary conditions at $t = T_B$. Specifically, we demand that both A and $\frac{\partial A}{\partial t}$ are continuous across the time boundary for any z. This requirement results in the following two equations:

$$\begin{aligned} &e^{i(\beta' z - \Delta\omega T_B)} + Re^{i(\beta'_r z - \Delta\omega_r T_B)} = Te^{i(\beta'_t z - \Delta\omega_t T_B)} \\ &- i\Delta\omega e^{i(\beta' z - \Delta\omega T_B)} - i\Delta\omega_r Re^{i(\beta'_r z - \Delta\omega_r T_B)} \\ &= -i\Delta\omega_t Te^{i(\beta'_t z - \Delta\omega_t T_B)}. \end{aligned} \quad (9)$$

Using $\beta' = \beta'_r = \beta'_t$ from Eq. (6), we obtain the following analytic expressions for R and T:

$$\begin{cases} R(\Delta\omega) = \frac{\Delta\omega_t - \Delta\omega}{\Delta\omega_r - \Delta\omega_t} e^{i(\Delta\omega_r - \Delta\omega)T_B} \\ T(\Delta\omega) = \frac{\Delta\omega_r - \Delta\omega}{\Delta\omega_r - \Delta\omega_t} e^{i(\Delta\omega_t - \Delta\omega)T_B} \end{cases}. \quad (10)$$

These expressions contain a linear phase shift that depends on the boundary's location T_B. This phase shift is not important and can be removed by choosing $T_B = 0$. However, R and T can still be complex quantities. Figure 1 shows how their moduli and phases vary as a function of the frequency shift ($\Delta\nu$) using the notation $R = |R|e^{i\phi(R)}$ and $T = |T|e^{i\phi(T)}$. The parameters we used are appropriate for an optical fiber acting as a dispersive medium [6] and have values $\Delta\beta_1 = 0.1$ ps/m, $\beta_2 = 5$ ps^2/km and $\beta_B = 0.5$ m^{-1}.

The most striking feature in Fig. 1 occurs near $\Delta\nu_c = \frac{\sqrt{2\beta_2\beta_B} - \Delta\beta_1}{2\pi\beta_2} = -0.93$ THz. When $\Delta\nu > \Delta\nu_c$, both R and T are real quantities. When $\Delta\nu < \Delta\nu_c$, they become complex.

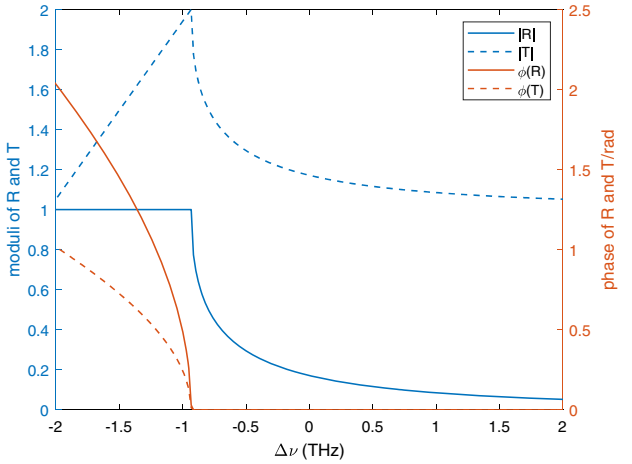

Fig. 1. Frequency dependence of the reflection and transmission coefficients for $\Delta\beta_1 = 0.1$ ps/m, $\beta_2 = 5$ ps^2/km and $\beta_B = 0.5$ m^{-1}. Solid and dashed curves show, respectively, the modulus and phase of these two quantities.

The reason for this change is related to the form of Eqs. (7) and (8). While $\Delta\omega_r$ is always real, $\Delta\omega_t$ can be complex depending on the sign of the discriminant in Eq. (8). The condition for this to happen is given by $(\Delta\beta_1 + \beta_2\Delta\omega)^2 < 2\beta_2\beta_B$. In this situation, $\Delta\omega_t$ becomes complex, and the transmitted wave becomes evanescent. It can be shown that $|R| = 1$ holds for $\Delta\omega < \Delta\omega_c$. This is the temporal analog of total internal reflection (TIR) discussed in Ref. [6]. We call $\Delta\nu_c$ the critical frequency. It will play an important role in Section 4.

The preceding discussion applies to each specific frequency component of a pulse. We can use it to study how an incident pulse gets reflected and transmitted at the temporal boundary. Consider an incident pulse with the slowly varying amplitude

$$A(z = 0,\, t) = A_{\text{in}}(t). \tag{11}$$

We can decompose it into plane waves of different frequencies using the Fourier transform:

$$\tilde{A}(\Delta\omega) = \int A_{\text{in}}(t) e^{i\Delta\omega t}\mathrm{d}t. \tag{12}$$

The evolution of each plane-wave component is governed by Eq. (4). The total field can be calculated by integrating over the input pulse's spectrum to obtain the following:

If $t < T_B$,

$$A(z,\, t) = \frac{1}{2\pi}\int \tilde{A}(\Delta\omega) e^{i(\beta'(\Delta\omega)z - \Delta\omega t)}\mathrm{d}\Delta\omega + \frac{1}{2\pi}\int \tilde{A}(\Delta\omega)\, R(\Delta\omega) e^{i(\beta_r'(\Delta\omega)z - \Delta\omega_r t)}\mathrm{d}\Delta\omega. \tag{13}$$

If $t > T_B$,

$$A(z,\, t) = \frac{1}{2\pi}\int \tilde{A}(\Delta\omega)\, T(\Delta\omega) e^{i(\beta_t'(\Delta\omega_t)z - \Delta\omega_t t)}\mathrm{d}\Delta\omega. \tag{14}$$

This is our main result. It is used to find the shapes and spectra of the reflected and transmitted parts of any input pulse.

To validate our analytic theory of temporal reflection and refraction, we consider a Gaussian pulse with the amplitude

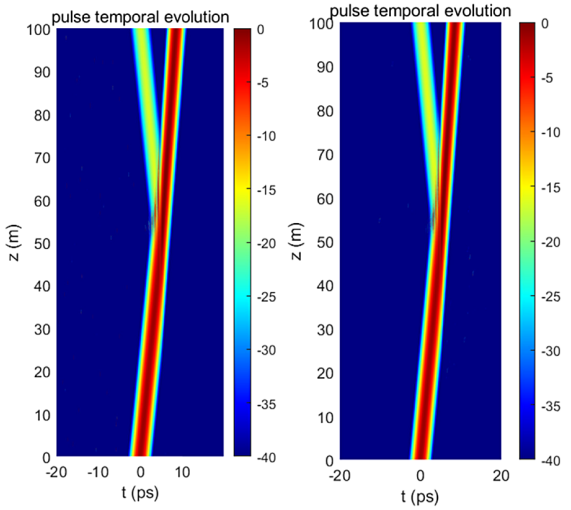

Fig. 2. Temporal reflection and refraction of 1-ps Gaussian pulses using the analytic reflection and transmission coefficients (left) and the split-step Fourier method (right). In both cases, the relative intensity $|A(z,\, t)|^2$ is plotted on a 40-dB scale.

$A_{\text{in}}(t) = e^{-\frac{1}{2}(t/T_w)^2}$ and choose $T_w = 1$ ps. This pulse is reflected at the boundary located at $T_B = 5$ ps as it propagates inside a dispersive medium. For the sake of comparison, we use the same parameters as those used in Ref. [6] and given in Fig. 1. We solved Eq. (3) numerically using the split-step Fourier method [23]. We also used our analytic theory to calculate the reflected and transmitted coefficients as a function of frequency and carry out the integrations in Eqs. (13) and (14). The results are compared in Fig. 2. As is evident, the two methods produce identical results and indicate that our analytical approach is valid. We stress at the reflected pulse is not moving backward because the results are shown in a moving frame. Rather, the incident pulse splits into two parts moving at different speeds such that the reflected part never crosses the boundary.

3. REFLECTED AND TRANSMITTED PULSES

In this section, we investigate the properties of reflected and transmitted pulses produced after a pulse with the amplitude $A_{\text{in}}(t)$ has arrived at the temporal boundary. From Eqs. (13) and (14), the reflected and transmitted fields are obtained using

$$A_r(z,\, t) = \frac{H(z - z_B)}{2\pi} \times \int \tilde{A}(\Delta\omega)\, R(\Delta\omega) e^{i\left(\beta_r'(\Delta\omega_r)z - \Delta\omega_r(\Delta\omega)t\right)}\mathrm{d}\Delta\omega, \tag{15}$$

$$A_t(z,\, t) = \frac{H(z - z_B)}{2\pi} \times \int \tilde{A}(\Delta\omega)\, T(\Delta\omega) e^{i\left(\beta_t'(\Delta\omega_t)z - \Delta\omega_t(\Delta\omega)t\right)}\mathrm{d}\Delta\omega, \tag{16}$$

where z_B is the distance when the pulse arrives at the temporal boundary. We have added the step function $H(z - z_B)$

because the reflected and transmitted pulses only exist after $z > z_B$. These integrals can be done numerically, but an analytic solution is not possible without some approximations.

One may ask if energy is conserved during temporal reflection. This is not easy to answer because a moving temporal boundary implies that another source of energy exists that was used to create a moving boundary (e.g., microwave radiation or a pump pulse). Here, we consider the intensity integral $\int |A_{\text{in}}(t)|^2 dt$ before and after the boundary to find the relation between the reflection and transmission coefficients. The condition $|R|^2 + |T|^2 = 1$ does not conserve the value of this integral. In this section, we use Eqs. (15) and (16) for the reflected and transmitted pulses to find the relation that conserves the intensity integral.

We assume that the incident pulse $A_{\text{in}}(t)$ has a narrowband spectrum with its central frequency at $\omega_0 + \Delta\omega_i$ where ω_0 is the reference frequency. Let $\Delta\omega$ be a variable that represents a plane-wave component at that frequency. We can understand the reflection at a temporal boundary using Fig. 3 [6], where we plot the parabolic dispersion curves, as defined by the approximation of the Taylor series expansion in Eq. (1), of the medium just before and after the temporal boundary (parameters used are the same as in Fig. 1).

We indicate in Fig. 3 the spectral range of the incident pulse by vertical dashed lines in region 1. The horizontal lines show the range of β' corresponding to this frequency range. The spectra of reflected and transmitted pulses correspond to the crossing points of horizontal lines with the dispersion curves because of the momentum conservation condition in Eq. (6). Ranges marked by 2 and 3 correspond to the spectra of reflected and transmitted pulses, respectively [6].

To find the Fourier amplitude of the reflected pulse, in Eq. (15) we change the integration variable from $\Delta\omega$ to $\Delta\omega_r$ to obtain

$$\tilde{A}_r(z, \Delta\omega_r) = \tilde{A}(\Delta\omega)\, R(\Delta\omega) e^{i\beta_r'(\Delta\omega_r)\mathbf{z}} \left| \frac{d\Delta\omega}{d\Delta\omega_r} \right|. \quad (17)$$

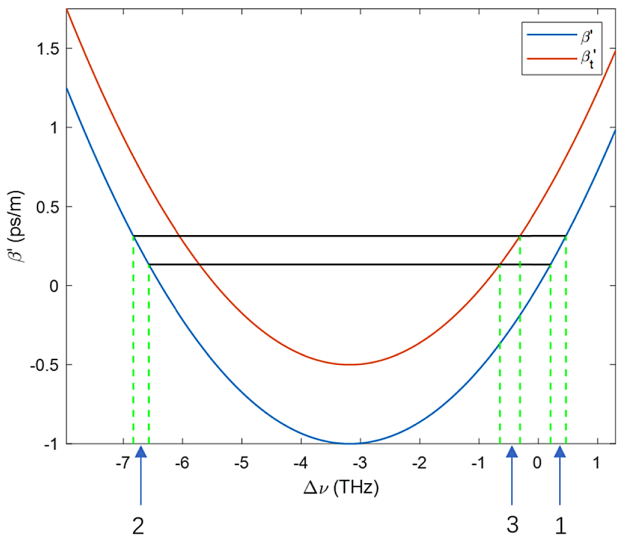

Fig. 3. Parabolic dispersion curves before (blue curve) and after (red curve) the time boundary. Vertical dashed lines (region 1) mark the spectral bandwidth of the incident pulse and horizontal lines show the range of β' in this frequency range. Regions 2 and 3 indicate the spectral range of the reflected and transmitted pulses.

The reason for the absolute value of $d\Delta\omega/d\Delta\omega_r$ is that when $d\Delta\omega/d\Delta\omega_r$ is negative, the integration interval must be flipped, which gives another minus sign. Similarly, the Fourier amplitude of the transmitted pulse can be written as

$$\tilde{A}_t(z, \Delta\omega_t) = \tilde{A}(\Delta\omega)\, T(\Delta\omega) e^{i\beta_t'(\Delta\omega_t)\mathbf{z}} \left| \frac{d\Delta\omega}{d\Delta\omega_t} \right|. \quad (18)$$

If the coefficients R and T vary slowly with $\Delta\omega$, which is the case in Fig. 1 when the central frequency of the pulse is far away from the TIR point, we can approximate both R and T with their values at the central frequency of the spectrum of the incident pulse:

$$\begin{cases} R(\Delta\omega) = R(\Delta\omega_i) = R_0 \\ T(\Delta\omega) = T(\Delta\omega_i) = T_0 \end{cases}. \quad (19)$$

From Eqs. (7) and (17), the spectrum of the reflected pulse is easily obtained:

$$\tilde{A}_r(z, \Delta\omega_r) = R_0 e^{i\beta_r'(\Delta\omega_r)\mathbf{z}} \tilde{A}\left(-\frac{2\Delta\beta_1}{\beta_2} - \Delta\omega_r \right), \quad (20)$$

where we used $d\Delta\omega_r = -d\Delta\omega$ from Eq. (7). This result shows that the spectrum of the reflected pulses is shifted by $-2\Delta\beta_1/\beta_2$. The shift can be on the red or the blue side, depending on the relative signs of the two dispersion parameters. The shape of the spectrum is a mirror image of the input spectrum, a feature that is seen only when the input spectrum is asymmetric.

The exponential term in the spectrum of the reflected pulse and the transmitted pulse will induce chirp and distortion when z becomes larger. This is the result of the propagation inside a dispersive medium and has nothing to do with the temporal reflection. To study the effect of temporal reflection alone, we consider a small segment near $z = z_B$. Before the temporal reflection, the Fourier amplitude of the incident pulse is $\tilde{A}(z_B, \Delta\omega)$, and the temporal amplitude is denoted $A_{\text{in}}(z_B, t)$. Then, we use the Fourier amplitude of the incident pulse just before the temporal reflection instead of the Fourier amplitude at $z = 0$. The phase term $e^{i\beta_r'(\Delta\omega_r)z}$ in Eq. (20) disappears because we are considering a small segment. Then, converting Eq. (20) back to time domain, we obtain

$$A_r(z_B, t) = R_0 e^{i\frac{2\Delta\beta_1}{\beta_2}t} A_{\text{in}}(z_B, -t). \quad (21)$$

It follows that the reflected pulse is a mirrored version of the pulse reaching the temporal boundary but with a reduced amplitude. Its energy is given by $|R_0|^2 E_p$, where E_p is energy of the input pulse.

The calculation for the transmitted pulse is more complicated because $\Delta\omega_t$ and $\Delta\omega$ do not have a linear relationship. For narrowband pulses, we can employ the Taylor expansion and, to the first order, $\Delta\omega_t$ and $\Delta\omega$ are linearly related as

$$\Delta\omega_t = \Delta\omega_t(\Delta\omega_i) + S\Delta\omega, \quad (22)$$

where $S = (d\Delta\omega_t/d\Delta\omega)|_{\Delta\omega=\Delta\omega_i}$ is the slope. Combining Eqs. (18) and (22), we have

$$\tilde{A}_t(z_B, \Delta\omega_t) = \frac{T_0}{S} \tilde{A}\left(z_B, \frac{\Delta\omega_t - \Delta\omega_t(\Delta\omega_i)}{S} \right). \quad (23)$$

By taking the inverse Fourier Theorem, we obtain the amplitude of the transmitted pulse in the form

$$A_t(z_B, t) = T_0 A(z_B, St) e^{-i\Delta\omega_t(\Delta\omega_i)t}. \tag{24}$$

To find an analytic expression for S, we consider the momentum conservation for the transmitted pulse. It follows from Eqs. (5) and (6) that

$$\Delta\beta_1\Delta\omega + \frac{\beta_2}{2}\Delta\omega^2 = \beta_B + \Delta\beta_1\Delta\omega_t + \frac{\beta_2}{2}\Delta\omega_t^2. \tag{25}$$

Taking the derivative with respect to $\Delta\omega$ on both sides, we obtain

$$S = \frac{\Delta\beta_1 + \beta_2\Delta\omega_i}{\Delta\beta_1 + \beta_2\Delta\omega_t(\Delta\omega_i)}. \tag{26}$$

Equation (24) shows that the temporal width of the transmitted pulse is reduced by a factor of S. This also follows from Eq. (23), which shows that the bandwidth of the transmitted pulse changes by a factor of S. As the fraction of energy that goes into the transmitted pulse is $|T_0|^2/S$, the conservation of energy integral requires

$$|R_0|^2 + \frac{|T_0|^2}{S} = 1. \tag{27}$$

We have verified that this relation is satisfied in all cases.

4. TWO EXAMPLES

In this section, we show two examples of temporal reflection and analyze them with our analytic theory to discuss the shapes and spectra of reflected and transmitted pulses. In the first case, the spectrum of incident pulse is far from the critical frequency in Fig. 1. We consider a Gaussian pulse with $A_{\text{in}}(t) = e^{-\frac{1}{2}(t/T_w)^2}$ and use $T_w = 1$ ps. Figure 4 shows the spectrum of this pulse, together with the reflection and transmission coefficients predicted by our theory using the parameter values given in Fig. 1

As seen in Fig. 4, the moduli of R and T are nearly constants over the bandwidth of the incident pulse. This is exactly the case we discussed in Section 3, so we expect the reflected pulse

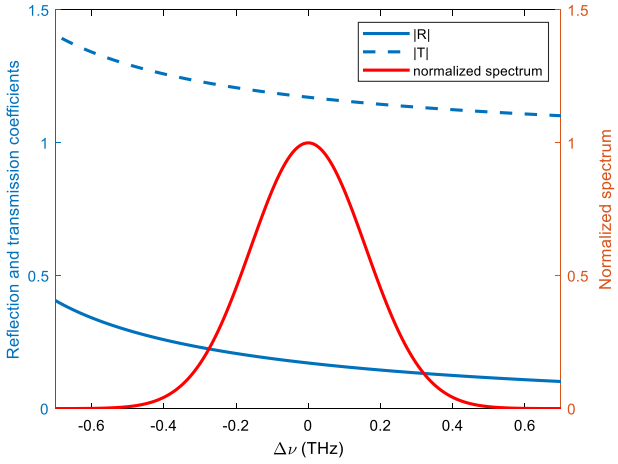

Fig. 4. Frequency dependence of $|R|$ and $|T|$. The spectrum of the incident pulse is also shown.

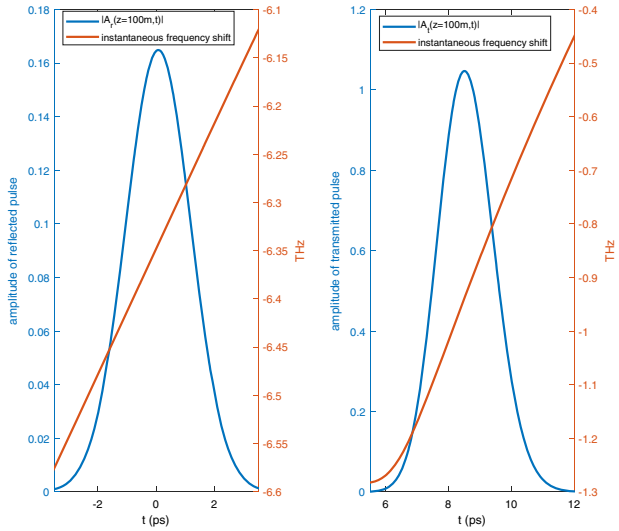

Fig. 5. Amplitude and instantaneous frequency shift of the reflected pulse and the transmitted pulse.

to have the same shape and width of the incident pulse, and the transmitted pulse to be slightly shorter. We plot in Fig. 5 the amplitudes of the reflected transmitted pulses at a distance of 100 m, obtained numerically using Eqs. (15) and (16).

Both the reflected and transmitted pulses retain the Gaussian shape of the input pulse but become chirped. We plot the time-dependent frequency shift obtained using [23]

$$\Delta\nu(t) = -\frac{1}{2\pi}\frac{d\phi}{dt}, \tag{28}$$

where $\phi(t)$ stands for the phase of $A(t)$. As seen in Fig. 5, the frequency chirp varies linearly for the reflected pulse and is almost linear for the transmitted pulse. We can write the chirp as $\Delta\nu(t) = \nu_0 + Ct$, where C is a constant. Because of the Gaussian shape of the pulses, we can theoretically predict the chirp coefficient using [23]

$$C = \frac{1}{2\pi}\frac{z/L_D}{T_w^2(1 + (z/L_D)^2)}, \tag{29}$$

where z is the propagation distance and $L_D = T_w^2/|\beta_2|$ is the dispersion length [23]. The slope of the chirp in Fig. 5 agrees with this analytical value of C. This agreement indicates that the pulse does not experience distortion when it splits into two parts at the temporal boundary, and the chirp is only from propagation inside the dispersive medium.

In the second example, we discuss the situation where the reflection and transmission coefficients cannot be treated as being constant over the pulse's bandwidth. In this case, a part of the spectrum of the incident pulse satisfies the TIR condition. We choose $\Delta\beta_1 = 0.07$ ps/m, $\beta_2 = 5$ ps^2/km, $\beta_B = 0.5$ m^{-1}. The incident pulse is still a Gaussian pulse with $T_w = 1$ ps and the temporal boundary is at $T_B = 5$ ps. Figure 6 shows the pulse's spectrum together with $|R|$ and $|T|$ as a function of $\Delta\nu$.

In this case, there is no good approximation for R and T. We calculate the reflected and transmitted pulse at $z = 200$ m by integrating Eqs. (15) and (16) numerically. Figure 7 shows the temporal (top) and spectral (bottom) amplitudes of the reflected

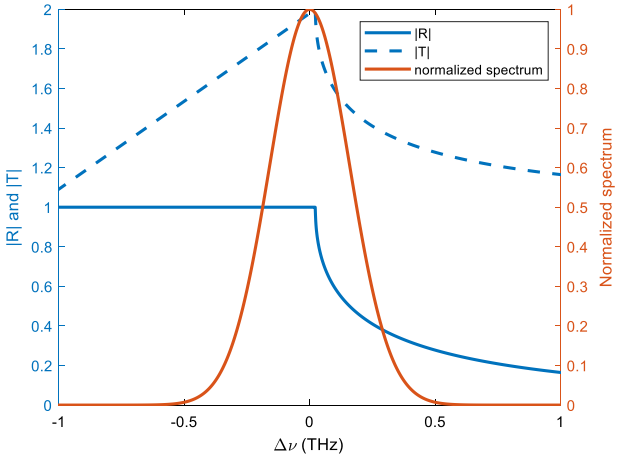

Fig. 6. Pulse spectrum and modulus of the reflection and transmission coefficients showing TIR over part of the spectrum.

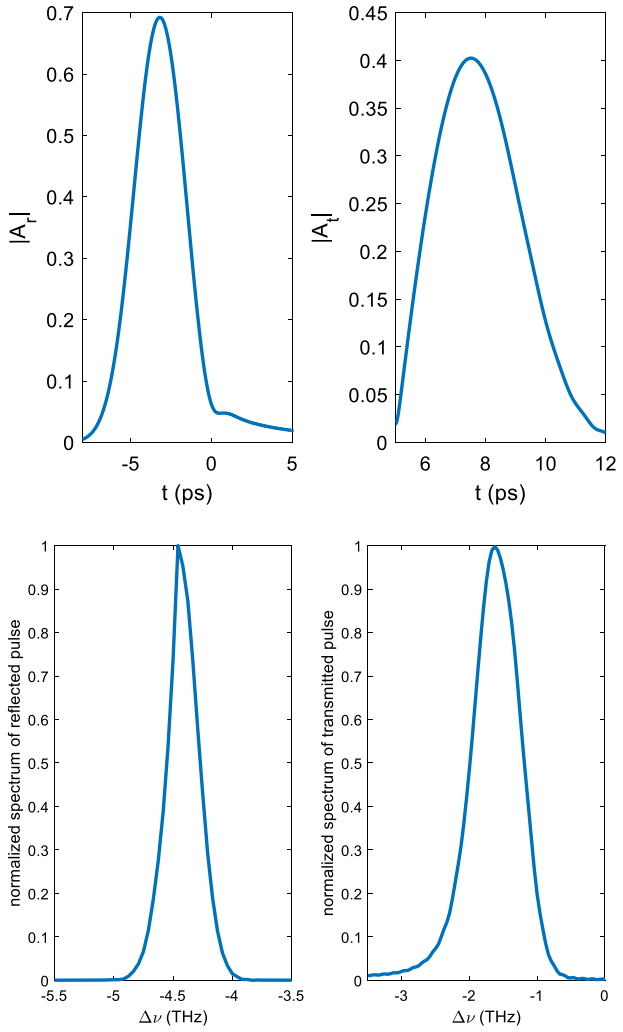

Fig. 7. Amplitudes (top) and spectra (bottom) of the reflected (left) and transmitted (right) pulses at $z = 200$ m.

and transmitted pulses, respectively. As seen there, both the reflected and transmitted pulses become asymmetric. The reflected pulse develops a long trailing edge, and the transmitted pulse's leading part is shorter than the trailing part. We can also see the distortion in their spectra. This is caused by the rapid change of $|R|$ and $|T|$ near the critical frequency. The distortion will be more severe for shorter pulses and pulses with sharper edges because their spectra are broader.

5. CONCLUSION

In this work, we have developed an analytical approach for studying the reflection and refraction of optical pulses at a temporal boundary inside a dispersive medium across which the refractive index changes by a relatively small amount. We decompose the incident pulses into its plane-wave spectral components and derive expressions for the reflection and transmission coefficients that depend on the frequency of the spectral component. Using the analytical results, we study the temporal reflection of an optical pulse and show that our results agree fully with a numerical approach used earlier.

Our approach also provides approximate analytic expressions for the electric fields of the reflected and transmitted pulses. Whereas the width of the transmitted pulse is modified, the reflected pulse is a mirror version of the incident pulse. We applied our analysis to a Gaussian pulse propagating inside an optical fiber. When a part of the incident spectrum lies in the region of total internal reflection, both the reflected and transmitted pulses are distorted considerably.

In practice, a moving temporal boundary can be created through the nonlinear Kerr effect by injecting an intense short pump pulse into an optical fiber in the region of anomalous GVD ($\beta_2 < 0$) and adjusting its energy such that it propagates as a fundamental soliton [23]. A probe pulse at a slightly different wavelength will be reflected at this pump-pulse-induced temporal boundary [22]. Such a pump-probe configuration provides an ideal situation to which our theoretical analysis can be applied.

Funding. National Science Foundation (ECCS-1933328).

Disclosures. The authors declare no conflicts of interest.

REFERENCES

1. J. T. Mendonça and P. K. Shukla, "Time refraction and time reflection: two basic concepts," Phys. Scr. **65**, 160–163 (2002).
2. M. Notomi and S. Mitsugi, "Wavelength conversion via dynamic refractive index tuning of a cavity," Phys. Rev. A **73**, 051803 (2006).
3. F. Biancalana, A. Amann, A. V. Uskov, and E. P. O'Reilly, "Dynamics of light propagation in spatiotemporal dielectric structures," Phys. Rev. E **75**, 046607 (2007).
4. N. N. Rozanov, "Transformation of electromagnetic radiation by rapidly moving inhomogeneities of a transparent medium," J. Exp. Theor. Phys. **108**, 140–148 (2009).
5. Y. Xiao, D. N. Maywar, and G. P. Agrawal, "Reflection and transmission of electromagnetic waves at a temporal boundary," Opt. Lett. **39**, 574–577 (2014).
6. B. W. Plansinis, W. R. Donaldson, and G. P. Agrawal, "What is the temporal analog of reflection and refraction of optical beams?" Phys. Rev. Lett. **115**, 183901 (2015).
7. D. K. Kalluri, *Electromagnetics of Time Varying Complex Media: Frequency and Polarization Transformer*, 2nd ed. (CRC Press, 2016).
8. C. Caloz and Z.-L. Deck-Léger, "Spacetime metamaterials—part I: general concepts," IEEE Trans. Antennas Propag. **68**, 1569–1582 (2020).

9. C. Caloz and Z.-L. Deck-Léger, "Spacetime metamaterials—part II: theory and applications," IEEE Trans. Antennas Propag. **68**, 1583–1598 (2020).
10. V. Pacheco-Peña and N. Engheta, "Temporal aiming," Light Sci. Appl. **9**, 129 (2020).
11. D. Ramaccia, A. Toscano, and F. Bilotti, "Light propagation through metamaterial temporal slabs: reflection, refraction, and special cases," Opt. Lett. **45**, 5836–5839 (2020).
12. A. V. Gorbach and D. V. Skryabin, "Bouncing of a dispersive pulse on an accelerating soliton and stepwise frequency conversion in optical fibers," Opt. Express **15**, 14560–14565 (2007).
13. S. Robertson and U. Leonhardt, "Frequency shifting at fiber-optical event horizons: the effect of Raman deceleration," Phys. Rev. A **81**, 063835 (2010).
14. L. Tartara, "Frequency shifting of femtosecond pulses by reflection at solitons," IEEE J. Quantum Electron. **48**, 1439–1442 (2012).
15. R. Driben, A. V. Yulin, A. Effmov, and B. A. Malomed, "Trapping of light in solitonic cavities and its role in the supercontinuum generation," Opt. Express **21**, 19091–19096 (2013).
16. S. F. Wang, A. Mussot, M. Conforti, X. L. Zeng, and A. Kudlinski, "Bouncing of a dispersive wave in a solitonic cage," Opt. Lett. **40**, 3320–3323 (2015).
17. B. W. Plansinis, W. R. Donaldson, and G. P. Agrawal, "Temporal waveguides for optical pulses," J. Opt. Soc. Am. B **33**, 1112–1119 (2016).
18. Z. Deng, X. Fu, J. Liu, C. Zhao, and S. Wen, "Trapping and controlling the dispersive wave within a solitonic well," Opt. Express **24**, 10302–10312 (2016).
19. B. W. Plansinis, W. R. Donaldson, and G. P. Agrawal, "Spectral splitting of optical pulses inside a dispersive medium at a temporal boundary," IEEE J. Quantum Electron. **52**, 6100708 (2016).
20. A. Antikainen, F. R. Arteaga-Sierra, and G. P. Agrawal, "Temporal reflection as a spectral broadening mechanism in dual-pumped dispersion-decreasing fibers and its connection to dispersive waves," Phys. Rev. A **95**, 033813 (2017).
21. B. W. Plansinis, W. R. Donaldson, and G. P. Agrawal, "Single-pulse interference caused by temporal reflection at a moving refractive-index boundary," J. Opt. Soc. Am. B **34**, 2274–2280 (2017).
22. B. W. Plansinis, W. R. Donaldson, and G. P. Agrawal, "Cross-phase-modulation-induced temporal reflection and waveguiding of optical pulses," J. Opt. Soc. Am. B **35**, 436–445 (2018).
23. G. P. Agrawal, *Nonlinear Fiber Optics*, 6th ed. (Academic, 2019), Chap. 3.